

EUROPEAN ORGANIZATION FOR NUCLEAR RESEARCH

Proposal to the ISOLDE and Neutron Time-of-Flight Committee

A study of seniority-2 configurations in $N = 126$ and 124 isotonic chains

January 2024

G. Rainovski¹, G. Georgiev², D. Kocheva¹, K. Gladnishki¹, M. Djongololov¹, K. Stoychev², N. Pietralla³, Th. Kröll³, V. Werner³, R. Zidarova³, T. Stetz³, H. Mayr³, A. Blazhev⁴, J. Jolie⁴, C. Fransen⁴, A. Esmaylzadeh⁴, N. Warr⁴, P. Reiter⁴, M. Droste⁴, H. Hess⁴, A.E. Stuchbery⁵, A.J. Mitchell⁵, G. Lane⁵, T. Kibedi⁵, B. Coombes⁵, Zs. Podolyák⁶, M. Scheck⁷, D.L. Balabanski⁸, T. Grahn⁹, J. Pakarinen⁹, G. De Gregorio^{10,11}, A. Gargano¹¹, T. Otsuka¹², B. Alex Brown¹³

¹ Faculty of Physics, St. Kliment Ohridski University of Sofia, 1164 Sofia, Bulgaria

² IJCLab, IN2P3/CNRS, and Université Paris-Saclay, F-91405 Orsay Campus, France

³ Institut für Kernphysik, Technische Universität Darmstadt, 64289 Darmstadt, Germany

⁴ Institut für Kernphysik, Universität zu Köln, 50937 Köln, Germany

⁵ Department of Nuclear Physics, The Australian National University, Canberra, Australia

⁶ University of Surrey, Guildford, UK

⁷ School of Engineering & Computing, University of the West of Scotland, Paisley PA1 2BE

⁸ ELI-NP, IFIN, Bucharest, Romania

⁹ University of Jyväskylä, Department of Physics, P.O. Box 35, FI-40014, Finland

¹⁰ Dipartimento di Matematica e Fisica, Università degli Studi della Campania "Luigi Vanvitelli", I-81100 Caserta, Italy

¹¹ INFN Sezione di Napoli, IT-80126 Napoli, Italy

¹² Department of Physics, The University of Tokyo, 7-3-1 Hongo, Bunkyo, Tokyo 113-0033, Japan

¹³ Michigan State University, East Lansing, Michigan 48824-1321

Spokespersons: G. Rainovski (rig@phys.uni-sofia.bg), G. Georgiev

(georgi.georgiev@ijclab.in2p3.fr)

Contact person: S. Freeman (sean.freeman@cern.ch)

Abstract: We propose to perform Coulomb excitation of the $^{214,212}\text{Ra}$ and the $^{212,210}\text{Rn}$ isotopes. This experiment consists of two separate runs aimed at measuring the $B(E2; 2^+_1 \rightarrow 0^+_{11})$ strengths in $^{214,212}\text{Ra}$ and in $^{212,210}\text{Rn}$ and, possibly, the $B(E2; 4^+_1 \rightarrow 2^+_{11})$ strengths in ^{212}Ra and ^{210}Rn . This experimental information will allow us to study quantitatively, within the framework of the nuclear shell model, to what extent the seniority scheme remains valid in the Po-Ra-Rn isotones with $N = 126$ and 124 .

Summary of requested shifts: 29 shifts, split into 2 runs over 2 years.



Physics case:

The Nuclear Shell Model is one of the most successful effective theories in nuclear structure physics [1]. Besides many other insights on the structure of nuclei, the shell model, in combination with pairing correlations, provides an easy way for understanding low-energy spectra of semi-magic nuclei. Low-energy excited states with $J > 0$ in semi-magic nuclei, with more than two-particles in a single high- j shell, originate from angular momenta recoupling of unpaired nucleons. These states can be grouped into multiplets based on the number of unpaired nucleons. This number is called seniority (ν) [2, 3] and can be considered as a good quantum number. In fact, the generalized seniority scheme [3] represents a truncation of the nuclear shell model. For the yrast states of even-even nuclei it is manifested by few clear experimental signatures [4, 5]:

- The excited yrast states have seniority $\nu = 2$ and follow an energy pattern that is equivalent to the one for a j^2 configuration in which the energy spacing between the states decreases towards the state with maximum angular momentum. As a result, the state with maximum angular momentum for the j^2 configuration is usually an isomer.
- The absolute $E2$ transition strength for the seniority-changing transition $2^+_{\nu=2} \rightarrow 0^+_{\nu=0}$ increases in a parabolic way with the filling of the j -shell and reaches a maximum at the middle of the j -shell.
- The absolute $E2$ transition strengths for the seniority-conserving transitions $J \rightarrow J-2$ ($J > 4$) decrease in a parabolic way with the filling of the j -shell and reaches a minimum at the middle of the j -shell.
- the middle of the j -shell.

The even-even Po-Rn-Ra nuclei with $N = 126$ manifest these features. The yrast states of ^{210}Po , ^{212}Rn , and ^{214}Ra adhere to the typical seniority-2 energy pattern (cf. Fig. 1).

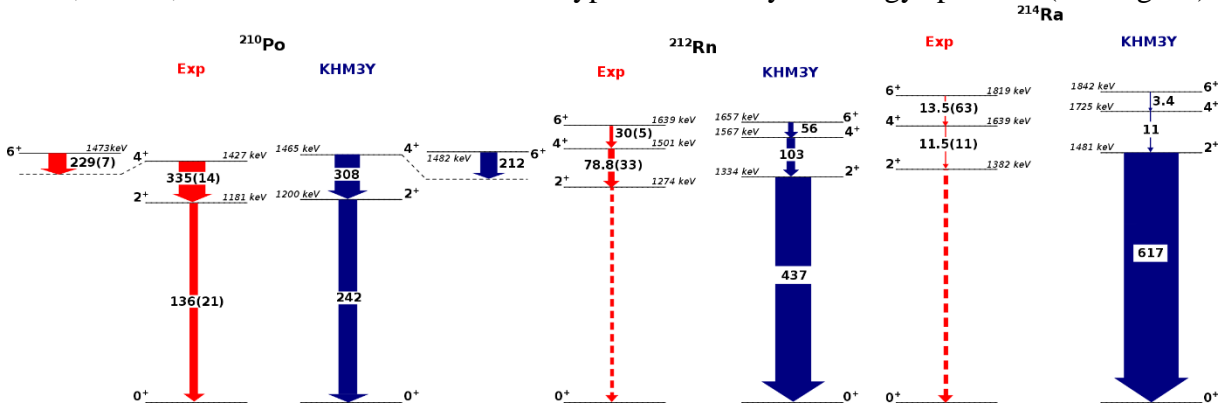


Figure 1: A graphical comparison between the experimental (Exp) and calculated (KHM3Y) properties of the yrast states of the $N = 126$ isotones ^{210}Po , ^{212}Rn , and ^{214}Ra . The isomeric $8^+_{\nu=1}$ states which are a few keV apart from the $6^+_{\nu=1}$ states, are intentionally omitted. The experimental data are taken from NNDC and the references therein. Details about the calculations are presented in the text. The thickness of the arrows is proportional to the $B(E2)$ values with the latter also indicated by the numbers on the arrows in e^2fm^4 . Dashed arrows represent transitions for which experimental data on $B(E2)$ values are not available.

This pattern can be attributed to the $\pi(1h_{9/2})^2$ configuration. This assignment agrees with the almost constant values of the measured magnetic moments of the $8^+_{\nu=1}$ states ^{210}Po , ^{212}Rn , and ^{214}Ra [6]. The predicted decreasing trend in the absolute $E2$ transition strengths for the seniority-preserving transitions is also evident in Fig. 2. *However, due to the lack of*

experimental data, the anticipated parabolically increasing trend in the absolute $E2$ transition strength for the seniority-changing transition from $2^+_{1}(v=2) \rightarrow 0^+_{1}(v=0)$ is still not experimentally observed.

It can be expected that the features of the seniority scheme persist in open shell nuclei close to magic numbers in which low-energy excitations are dominated by one kind of nucleons. The

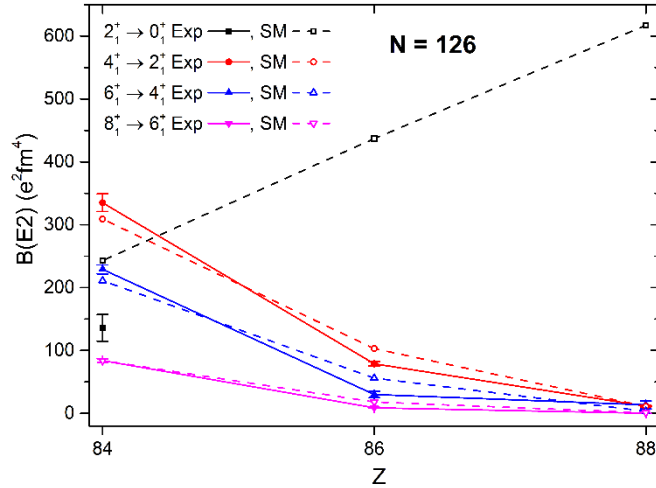


Figure 2: A comparison between the experimental (filled symbols) and the calculated (opened symbols) $B(E2)$ strengths for the transitions between the yrast states of the $N = 126$ isotones ^{210}Po , ^{212}Rn , and ^{214}Ra . The experimental data are taken from NNDC and the references therein. Details about the calculations are presented in the text. The lines are drawn to guide the eye.

valence neutrons in $N < 126$ nuclei occupy orbitals with high principal quantum number and low angular momentum. As a result, they interact weakly with the protons in the $1h_{9/2}$ orbital [7]. Therefore, the protons in the $1h_{9/2}$ orbital dominate the wave functions of the yrast states forming seniority-like structures. Indeed, for all even-even nuclei in the Po-Rn-Ra isotonic chains with $N = 124$ the yrast states follow a typical seniority-like pattern (cf. Fig. 3). The 8^+_{1}

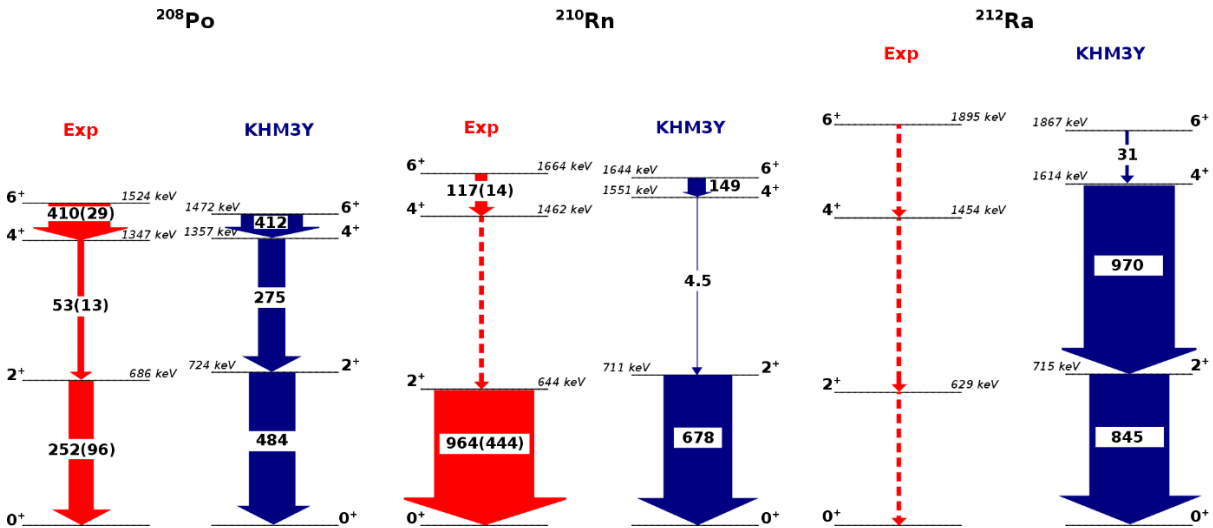


Figure 3: A graphical comparison between the experimental (Exp) and calculated (KHM3Y) properties of the yrast states of the $N = 124$ isotones ^{208}Po , ^{210}Rn , and ^{212}Ra . The isomeric 8^+_{1} states which are a few keV apart from the 6^+_{1} states, are intentionally omitted. The experimental data are taken from NNDC and the references therein. Details about the calculations are presented in the text. The thickness of the arrows is proportional to the $B(E2)$ values with the latter also indicated by the numbers on the arrows in e^2fm^4 . Dashed arrows represent transitions for which experimental data on $B(E2)$ values are not available.

states in these nuclei are isomers with almost constant values of the measured magnetic moments [6] which indicate wave functions dominated by the $\pi(1h_{9/2})^2$ configuration [8]. Based on these and similar arguments J.J. Ressler *et al.* [5] suggested that the seniority regime persists

for nuclei from the Po-Rn-Ra isotonic chains with $122 \leq N \leq 126$ up to ^{210}Ra [8]. On the other hand, the evolution of the absolute $E2$ transition strengths with the increase in the proton number is not entirely clear (cf. also Fig. 4). Indeed, the $B(E2; 2^+_{11} \rightarrow 0^+_{11})$ values increase from ^{208}Po to ^{210}Rn while the $B(E2; 6^+_{11} \rightarrow 4^+_{11})$ values decrease. **However, the $B(E2; 2^+_{11} \rightarrow 0^+_{11})$ in ^{210}Rn is quite uncertain [9], and no further experimental information on the $E2$ transition strengths in ^{210}Rn and ^{212}Ra is available.**

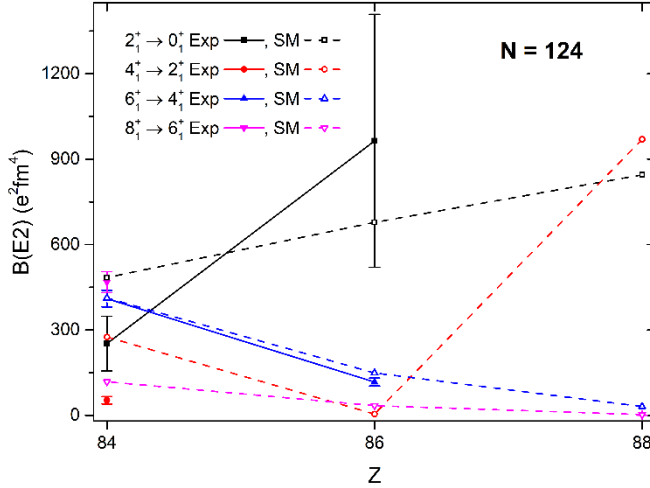


Figure 4: A comparison between the experimental (filled symbols) and the calculated (opened symbols) $B(E2)$ strengths for the transitions between the yrast states of the $N = 124$ isotones ^{208}Po , ^{210}Rn , and ^{212}Ra . The experimental data are taken from NNDC and the references therein. Details about the calculations are presented in the text. The lines are drawn to guide the eye.

In order to assess the capability of shell models to describe the observed properties of the yrast states of Po-Rn-Ra isotopes with $N = 126$ and 124 , we have performed calculations by considering ^{208}Pb as a core and by using the model space spanned by the $2p_{3/2}$, $2p_{1/2}$, $1f_{7/2}$, $1f_{5/2}$, $0h_{9/2}$, $0i_{13/2}$ orbitals for both protons and neutrons. For the two-body matrix elements of the effective Hamiltonian, we employed the KHM3Y interaction [10] which has recently been successfully applied to describe the yrast properties of ^{206}Po [11]. The results (henceforth labeled as KHM3Y or SM in Figures 1, 2, 3, and 4) were obtained using the shell-model code KSHELL [12]. To calculate the electromagnetic properties of the yrast states of Po-Rn-Ra isotopes with $N = 126$ and 124 , we employed effective charges of $e_{\pi} = 1.45e$ and $e_{\nu} = 0.84e$, which were chosen to reproduce the experimental values of $B(E2; 8^+_{11} \rightarrow 6^+_{11})$ in ^{210}Po and $B(E2; 2^+_{11} \rightarrow 0^+_{11})$ in ^{206}Pb , respectively. For effective gyromagnetic factors, we adopted the values recommended in Ref. [13]. With this choice of effective gyromagnetic factors, the calculations **successfully reproduce the experimental magnetic moments of the 8^+_{11} states of Po-Rn-Ra isotopes with $N = 126$ and 124 .** The other results are presented in Figures 1, 2, 3, and 4.

A comparison between the experimental and calculated spectra of the yrast states of Po-Rn-Ra isotopes with $N = 126$ is shown in Fig. 1. The calculated excitation energies of the yrast states are in very good agreement with the experimental data, with discrepancies less than 100 keV for all states. The description of ^{210}Po is particularly good, with discrepancies less than 38 keV. This is also true for the $E2$ transition strengths in ^{210}Po as all experimental strengths but $B(E2; 2^+_{11} \rightarrow 0^+_{11})$ are well reproduced (see Fig. 2). The latter is predicted by the calculations to be about twice as much as the experimental value [14]. This problem is well known and is being addressed in the IS720 experiment. The present shell model calculations predict that the $E2$ transition strengths between the yrast states of Po-Rn-Ra isotopes with $N = 126$ will follow the expected seniority pattern (see Fig. 2). The agreement between the calculated and the experimental $E2$ transition strengths for the seniority-preserving transitions is fairly good. However, such a comparison is not possible for the $E2$ transition strengths for the seniority-

changing transitions due to the lack of experimental data on $B(E2; 2^+_1 \rightarrow 0^+_1)$ in ^{212}Rn and ^{214}Ra . ***While it can be anticipated that these transition strengths will qualitatively follow the expected seniority pattern in accordance with current shell model calculations, the extent to which quantitative agreement can be achieved remains uncertain. In other words, it is unclear whether the observed discrepancy between the experimental and the calculated $B(E2; 2^+_1 \rightarrow 0^+_1)$ values in ^{210}Po persists or is reduced in ^{212}Rn and ^{214}Ra . Therefore, one of the objectives of the present proposal is to measure the $B(E2; 2^+_1 \rightarrow 0^+_1)$ strengths in ^{212}Rn and ^{214}Ra using the safe Coulomb excitation technique of radioactive ion beams.***

A comparison between the experimental and calculated spectra of the yrast states of Po-Rn-Ra isotopes with $N = 124$ is shown in Figure 3. The agreement between the calculated excitation energies of the yrast states and the experimental data is not as good as in the case of $N = 126$ isotones, as the largest discrepancy of 160 keV appears for the 4^+_1 state of ^{212}Ra . Moreover, the calculated 6^+_1 and 8^+_1 states systematically appear below the experimental ones. This indicates certain deficiencies in the effective interaction, most likely related to the proton-neutron two-body matrix elements, as discussed in Refs. [14, 15]. The comparison between the calculated and the experimental $E2$ transition strengths (see also Fig. 4) offers another peculiar observation: while the experimental $B(E2; 6^+_1 \rightarrow 4^+_1)$ values are well reproduced, the $B(E2; 2^+_1 \rightarrow 0^+_1)$ and $B(E2; 4^+_1 \rightarrow 2^+_1)$ values are overpredicted by a factor of two, and the experimental $B(E2; 8^+_1 \rightarrow 6^+_1)$ value is underpredicted by a factor of four. It is worth mentioning that by using different interactions, the discrepancy in the $B(E2; 4^+_1 \rightarrow 2^+_1)$ values may be amended, but those in the $B(E2; 2^+_1 \rightarrow 0^+_1)$ and $B(E2; 8^+_1 \rightarrow 6^+_1)$ values persist (see Table II in Ref. [15]). The present shell model calculations predict that the $E2$ transition strengths between the yrast states of Po-Rn-Ra isotopes with $N = 124$ will follow the expected seniority pattern (see Fig. 4). Indeed, both calculated and experimental $B(E2; 6^+_1 \rightarrow 4^+_1)$ values *decrease* from ^{208}Po to ^{210}Rn in good quantitative agreement. The experimental and the calculated $B(E2; 2^+_1 \rightarrow 0^+_1)$ increase in a qualitative agreement but it is *difficult to quantify this agreement due to the rather uncertain $B(E2; 2^+_1 \rightarrow 0^+_1)$ value in ^{210}Rn* [9]. Going from ^{210}Rn to ^{212}Ra , the current shell model calculations predict that all $E2$ transition strengths, except for the $B(E2; 4^+_1 \rightarrow 2^+_1)$, follow the seniority pattern. For the $B(E2; 4^+_1 \rightarrow 2^+_1)$ value in ^{212}Ra , a sudden increase is predicted (see Fig. 4), which may be an indication of onset of collectivity. *However, neither of these predictions can be verified due to the lack of experimental data on the $E2$ transition strengths in ^{212}Ra . Therefore, another objective of the present proposal is to measure the $B(E2; 2^+_1 \rightarrow 0^+_1)$ and the $B(E2; 4^+_1 \rightarrow 2^+_1)$ strengths in ^{210}Rn and ^{212}Ra using the safe Coulomb excitation technique of radioactive ion beams.*

In summary, the objectives of this proposal are to measure the $B(E2; 2^+_1 \rightarrow 0^+_1)$ strengths in $^{212,210}\text{Rn}$ and in $^{214,212}\text{Ra}$ and, potentially, the $B(E2; 4^+_1 \rightarrow 2^+_1)$ strengths in ^{210}Rn and ^{212}Ra . This experimental information will allow us to study quantitatively, within the framework of nuclear shell model, to what extent the seniority scheme remains valid as the number of nucleons diverges from (semi-)magic numbers.

Feasibility of the proposed experiment

The proposed measurements can be done in two separate runs, each devoted to $^{214,212}\text{Ra}$ and $^{212,210}\text{Rn}$, respectively. Radioactive ion beams of $^{214,212}\text{Ra}$ and $^{212,210}\text{Rn}$ can be produced at ISOLDE and post-accelerated by HIE-ISOLDE.

The ^{212}Rn and ^{210}Rn beams can be produced using uranium or thorium targets and cold-plasma ion source (VD7). This should provide sufficiently pure beams (without any surface-ionized francium contamination) with ISOLDE intensities of the order of 3×10^8 p/uC. Assuming an overall HIE-ISOLDE efficiency (charge breeding and post-acceleration) of about 5% should allow obtaining about 1×10^7 pps on the Miniball target. However, in the following estimates we have used a secondary beam intensity of 1×10^6 pps as a (conservative) value that could be accepted at the Miniball setup.

The production of the $^{212,214}\text{Ra}$ beams might appear more complex. Ra could be extracted from the ISOLDE target either by using surface ionization or using the RILIS ion source. The second option should allow for increasing the ionization efficiency by a factor of 3.8 [16]. The yields for ^{212}Ra and ^{214}Ra are cited as 9×10^6 p/uC (values from SC measurements). However, more recent PSB values are almost a factor of 20 lower (5×10^5 p/uC). Those are the numbers we used in our further beam intensity estimates.

The francium surface ionization contamination needs to be considered in either of the two ionization options. The very short half-life of ^{214}Fr (5 ms) suppresses it considerably and it should be reduced by many orders of magnitude lower intensity, compared to ^{214}Ra . Therefore, the ^{214}Fr contamination in either of the two ionization approaches could be considered as negligible and no specific precautions need to be taken in this case. The half-life of ^{212}Fr is very similar to that of ^{212}Ra and its intensity is expected to be several orders of magnitude higher than ^{212}Ra . Therefore, for the case of ^{212}Ra , we would like to go for extracting ^{212}RaF (mass 231) molecular beam. For this purpose, we will need a ThCx target, from which the ^{231}Fr will not be produced (it has two neutrons more than ^{232}Th).

In short, for ^{214}Ra we would like to use a ThCx target with RILIS ionization and we would assume 5×10^5 p/uC yield from ISOLDE. The same target will be used for the ^{212}Ra beam, however, extracting ^{212}RaF (mass 231) molecular beam. The yields for ^{212}RaF beam are expected to be about 2×10^5 p/uC. Both those options would allow extracting sufficiently pure ^{212}Ra and ^{214}Ra beams. Assuming proton beam intensity of 2 uA and 5% HIE-ISOLDE efficiency we expect 5×10^4 pps ^{214}Ra and 2×10^4 pps ^{212}Ra beams on the Miniball target. The breaking of the ^{212}RaF molecule will be done in the EBIS without any loss of overall efficiency.

Putting the numbers all together gives **5×10^4 pps ^{214}Ra , 2×10^4 pps ^{212}Ra and 1×10^6 pps for $^{212,210}\text{Rn}$** on the Miniball target.

Count rate estimates:

The beams of ^{214}Ra , ^{212}Ra , ^{212}Rn , and ^{210}Rn will be excited on a 2 mg/cm^2 ^{120}Sn target. The beam energy for all isotopes is chosen to be 4.5 MeV/u to ensure safe Coulomb excitation [17]. The proposed reaction is in inverse kinematics (cf. Fig. 5). The DSSD will be placed 20 mm behind the target covering scattering angles between 24° and 62° in the laboratory system. As can be seen in Fig. 5, the beam and the target particles can be well distinguished for all angles in the DSSD above 27° .

^{214}Ra case – the count rate estimates are based on a beam intensity delivered at Miniball of 5×10^4 pps. We have assumed a $B(E2; 2^+_1 \rightarrow 0^+_1) = 308 \text{ e}^2\text{fm}^4$ which corresponds to a half of the predicted value (see Fig. 1). The transition energy of interest is 1382 keV for which we assume a Miniball efficiency of 4%. Under these conditions it can be expected ***261 counts per day (3 shifts) in the $2^+_1 \rightarrow 0^+_1$ gamma line*** which will provide 6% statistical uncertainty for the determination of the $B(E2; 2^+_1 \rightarrow 0^+_1)$.

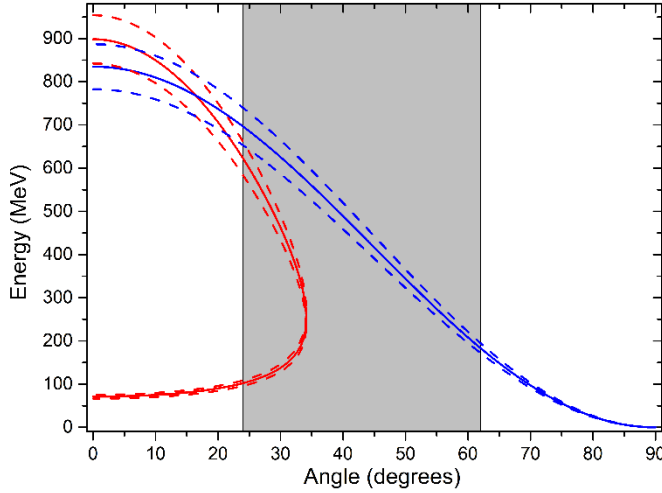


Figure 5: Reaction kinematics for 4.5 MeV/u ^{212}Rn (red) on a 2 mg/cm^2 ^{120}Sn target (blue). The shaded area indicates the angular coverage of the particle detector.

^{212}Ra case – the count rate estimates are based on a beam intensity delivered at Miniball of 2×10^4 pps. We have assumed a $B(E2; 2^+_1 \rightarrow 0^+_1) = 422\text{ e}^2\text{fm}^4$ and a $B(E2; 4^+_1 \rightarrow 2^+_1) = 485\text{ e}^2\text{fm}^4$ which correspond to a half of the predicted values (see Fig. 2). The transition energies of interest are 629 keV and 825 keV for which we assume Miniball efficiencies of 10% and 8%, respectively. Under these conditions it can be expected **1407 gammas per day (3 shifts) in the $2^+_1 \rightarrow 0^+_1$ gamma line** and **21 gammas per day in the $4^+_1 \rightarrow 2^+_1$ gamma line**. Thus, for 3 days, the prediction for a large $B(E2; 4^+_1 \rightarrow 2^+_1)$ can be checked with a statistical uncertainty of 13%.

^{212}Rn case – the count rate estimates are based on a beam intensity delivered at Miniball of 10^6 pps. We have assumed a $B(E2; 2^+_1 \rightarrow 0^+_1) = 218\text{ e}^2\text{fm}^4$ which corresponds to a half of the predicted value (see Fig. 1). The transition energy of interest is 1274 keV for which we assume Miniball efficiencies of 7%. Under these conditions it can be expected **3084 counts per shift (8 hours) in the $2^+_1 \rightarrow 0^+_1$ gamma line**.

^{210}Rn case – the count rate estimates are based on a beam intensity delivered at Miniball of 10^6 pps. We have assumed a $B(E2; 2^+_1 \rightarrow 0^+_1) = 520\text{ e}^2\text{fm}^4$ which corresponds to lower limit of the adopted experimental value (see Fig. 2 and Ref. [9]). For the $B(E2; 4^+_1 \rightarrow 2^+_1)$ we have assumed a value of $5\text{ e}^2\text{fm}^4$ which corresponds to the predicted value (see Fig. 2). The transition energies of interest are 643 keV and 817 keV for which we assume Miniball efficiencies of 10% and 8%, respectively. Under these conditions it can be expected **30240 counts per shift in the $2^+_1 \rightarrow 0^+_1$ gamma line** and **15 counts per day in the $4^+_1 \rightarrow 2^+_1$ gamma line**. Thus, for 4 days a statistical uncertainty of 13% can be achieved for the $4^+_1 \rightarrow 2^+_1$ gamma line.

In summary, we apply for two runs which consist of **14** and **15** shifts as follow:

Run 1 ^{214}Ra & ^{212}Ra (14 shifts – 5 days) - the shifts are distributed as follow:

- 1 shift for tuning ^{214}Rn beam;
- 3 shifts for ^{214}Ra beam at 4.5 MeV/u on a 2 mg/cm^2 ^{120}Sn target;
- 1 shift for tuning ^{212}Rn beam;
- 9 shifts for ^{212}Ra beam at 4.5 MeV/u on a 2 mg/cm^2 ^{120}Sn target.

Run 2 ^{212}Rn & ^{210}Rn (15 shifts – 5 days) - the shifts are distributed as follow:

- 1 shift for tuning ^{212}Rn beam;
- 1 shift for ^{212}Rn beam at 4.5 MeV/u on a 2 mg/cm^2 ^{120}Sn target;
- 1 shift for tuning ^{210}Rn beam;
- 12 shifts for ^{210}Ra beam at 4.5 MeV/u on a 2 mg/cm^2 ^{120}Sn target.

References:

- [1] Maria Goeppert Mayer, Phys. Rev. **78**, 16 (1950).
- [2] A. de Shalit and I. Talmi, *Nuclear Shell Theory* (Academic Press, New York, 1963).
- [3] Igal Talmi, Nucl. Phys. A **172**, 1 (1971).
- [4] R. F. Casten, *Nuclear Structure from a Simple Perspective* (Oxford University Press, New York, 2000).
- [5] J.J. Ressler *et al.*, Phys. Rev. C **69**, 034317 (2004) *and the references therein*.
- [6] N.J. Stone, At. Data Nucl. Data Tables **90**, 75 (2005).
- [7] K. Heyde *et al.*, Nucl. Phys. **A466**, 189 (1987).
- [8] J.J. Ressler *et al.*, Phys. Rev. C **69**, 034331 (2004).
- [9] T. Grahn *et al.*, Eur. Phys. J. A **52**, 340 (2016).
- [10] B. A. Brown, Phys. Rev. Lett. **85**, 5300 (2000).
- [11] D. Kocheva *et al.*, *in print* Physica Scripta (2024).
- [12] N. Shimizu, T. Mizusaki, T. Utsuno, and Y. Tsunoda, Comput. Phys. Commun. **244**, 372 (2019).
- [13] I.S. Towner, Physics Reports **155**, 263 (1987).
- [14] D. Kocheva *et al.*, Eur. Phys. J. **A53**, 175 (2017).
- [15] D. Kalaydjieva *et al.*, Phys. Rev. C **104**, 024311 (2021).
- [16] <https://riliselements.web.cern.ch/index.php?element=Ra>.
- [17] D. Cline Annu. Rev. Nucl. Part. Sci. **36**, 683 (1986).

1 Details for the Technical Advisory Committee

3.1 General information

Describe the setup which will be used for the measurement. If necessary, copy the list for each setup used.

- Permanent ISOLDE setup: *Name (e.g. CRIS, IDS, Miniball, etc.)*
 - To be used without any modification
 - To be modified: *Short description of required modifications.*
- Travelling setup (*Contact the ISOLDE physics coordinator with details.*)
 - Existing setup, used previously at ISOLDE: *Specify name and IS-number(s)*
 - Existing setup, not yet used at ISOLDE: *Short description*
 - New setup: *Short description*

3.2 Beam production

For any inquiries related to this matter, reach out to the target team and/or RILIS (please do not wait until the last minute!). For Letters of Intent focusing on element (or isotope) specific beam development, this section can be filled in more loosely.

- Requested beams:

Isotope	Production yield in focal point of the separator ($/\mu\text{C}$)	Minimum required rate at experiment (pps)	$t_{1/2}$
^{210}Rn	3×10^8	1×10^6	2.4 h
^{212}Rn	3×10^8	1×10^6	24 m
^{212}Ra	2×10^5	2×10^4	13 s
^{214}Ra	5×10^5	5×10^4	2.5 s

- Full reference of yield information (*e.g. yield database, elog entry, previous experiment number, extrapolation and/or justified scaling factors, target number*)
- Target - ion source combination:
 - ^{212}Rn and ^{210}Rn - UCx or ThCx and cold plasma ion source
 - ^{212}Ra – ThCx target and RILIS ion source (3.8 times higher efficiency with RILIS compared to surface ionization: <https://riliselements.web.cern.ch/?element=Ra>)
 - ^{214}Ra – ThCx target and surface ionization using RaF (mass 231) molecule

- RILIS? (*No/Yes/for element A but not for element B*)
 - Yes, for ^{214}Ra only; No isomer selectivity nor LIST or PI-LIST modes
- Additional features?
 - Neutron converter: (*for isotopes 1, 2 but not for isotope 3.*)
 - Other: (*quartz transfer line, gas leak for molecular beams, prototype target, etc.*)
- Expected contaminants: *Isotopes and yields*
 - no contaminants foreseen for ^{210}Rn and ^{212}Rn ;
 - ^{214}Ra – negligible contamination from ^{214}Fr – (5×10^5 /uC for ^{214}Ra vs. 9×10^2 /uC for ^{214}Fr)
 - ^{212}Ra – no Francium contamination foreseen if ThCx target and RaF molecule used (^{231}Fr has 2 neutrons more than ^{232}Th)
- Acceptable level of contaminants: (*Not sensitive to stable contaminants, limited by ISCOOL overfilling, etc.*)
- Can the experiment accept molecular beams?
 - molecular beam requested for ^{212}Ra ;
 - molecular beam could be acceptable for ^{214}Ra , if the yields are higher than 5×10^5 /uC
- Are there any potential synergies (same element/isotope) with other proposals and LOIs that you are aware of?

3.3 HIE-ISOLDE

For any inquiries related to this matter, reach out to the ISOLDE machine supervisors (please do not wait until the last minute!).

- HIE ISOLDE Energy: (*MeV/u*); (*exact energy or acceptable energy range*)
 - Precise energy determination required
 - Requires stable beam from REX-EBIS for calibration/setup? *Isotope?*
- REX-EBIS timing
 - Slow extraction
 - Other timing requests

- Which beam diagnostics are available in the setup?
- standard Miniball diagnostics
- What is the vacuum level achievable in your setup?
- standard Miniball vacuum

3.4 Shift breakdown

The beam request only includes the shifts requiring radioactive beam, but, for practical purposes, an overview of all the shifts is requested here. Don't forget to include:

- Isotopes/isomers for which the yield need to be determined
- Shifts requiring stable beam (indicate which isotopes, if important) for setup, calibration, etc. Also include if stable beam from the REX-EBIS is required.

An example can be found below, please adapt to your needs. Copy the table if the beam time request is split over several runs.

Summary of requested shifts:

With protons	Requested shifts
Yield measurements for ^{212}Ra and ^{214}Ra	1 shift
Beam tuning for ^{212}Ra and ^{214}Ra	2 shifts
Data taking, ^{214}Ra	3 shifts
Data taking, ^{212}Ra	9 shifts
---	---
Beam tuning for ^{210}Rn and ^{212}Rn	2 shifts
Data taking, ^{212}Rn	1 shift
Data taking, ^{210}Rn	12 shifts

3.5 Health, Safety and Environmental aspects

3.5.1 Radiation Protection

- If radioactive sources are required:
 - Purpose?
 - Isotopic composition?
 - Activity?
 - Sealed/unsealed?

- For collections:
 - Number of samples?
 - Activity/atoms implanted per sample?
 - Post-collection activities? (*handling, measurements, shipping, etc.*)

3.5.2 Only for traveling setups

- Design and manufacturing
 - Consists of standard equipment supplied by a manufacturer
 - CERN/collaboration responsible for the design and/or manufacturing

- Describe the hazards generated by the experiment:

Domain	Hazards/Hazardous Activities		Description
Mechanical Safety	Pressure	<input type="checkbox"/>	[pressure] [bar], [volume][l]
	Vacuum	<input type="checkbox"/>	
	Machine tools	<input type="checkbox"/>	
	Mechanical energy (moving parts)	<input type="checkbox"/>	
	Hot/Cold surfaces	<input type="checkbox"/>	
Cryogenic Safety	Cryogenic fluid	<input type="checkbox"/>	[fluid] [m3]

Electrical Safety	Electrical equipment and installations	<input type="checkbox"/>	[voltage] [V], [current] [A]
	High Voltage equipment	<input type="checkbox"/>	[voltage] [V]
Chemical Safety	CMR (carcinogens, mutagens and toxic to reproduction)	<input type="checkbox"/>	[fluid], [quantity]
	Toxic/Irritant	<input type="checkbox"/>	[fluid], [quantity]
	Corrosive	<input type="checkbox"/>	[fluid], [quantity]
	Oxidizing	<input type="checkbox"/>	[fluid], [quantity]
	Flammable/Potentially explosive atmospheres	<input type="checkbox"/>	[fluid], [quantity]
	Dangerous for the environment	<input type="checkbox"/>	[fluid], [quantity]
	Laser	<input type="checkbox"/>	[laser], [class]

Non-ionizing radiation Safety	UV light	<input type="checkbox"/>	
	Magnetic field	<input type="checkbox"/>	[magnetic field] [T]
Workplace	Excessive noise	<input type="checkbox"/>	
	Working outside normal working hours	<input type="checkbox"/>	
	Working at height (climbing platforms, etc.)	<input type="checkbox"/>	
	Outdoor activities	<input type="checkbox"/>	
Fire Safety	Ignition sources	<input type="checkbox"/>	
	Combustible Materials	<input type="checkbox"/>	
	Hot Work (e.g. welding, grinding)	<input type="checkbox"/>	
Other hazards			